

Self-similar wave produced by local perturbation of the Kelvin-Helmholtz shear-layer instability

Jérôme Hoepffner,* Ralf Blumenthal, and Stéphane Zaleski

*Institut Jean le Rond D'Alembert, UMR 7190,
Université Pierre et Marie Curie, Paris, France.*

(Dated: January 15, 2011)

We show that the Kelvin-Helmholtz instability excited by a localized perturbation yields a self-similar wave. The instability of the mixing layer was first conceived by Helmholtz as the inevitable growth of any localized irregularity into a spiral, but the search and uncovering of the resulting self-similar evolution was hindered by the technical success of Kelvin's wavelike perturbation theory. The identification of a self-similar solution is useful since its specific structure is witness of a subtle nonlinear equilibrium among the forces involved. By simulating numerically the Navier-Stokes equations, we analyze the properties of the wave: growth rate, propagation speed and the dependency of its shape upon the density ratio of the two phases of the mixing layer.

PACS numbers: 47.20.Ft

Wind over water yields waves. Similarly, a liquid jet destabilizes and atomizes into a cloud of droplets. This mechanism is the shear-layer instability. Herman Ludwig von Helmholtz in 1868 publishes a controversial approach to fluid dynamics where surfaces of discontinuity play a central role [1]. He makes use of the recent theories of complex variables to manage his singular fields within the differential framework of the Euler equation. The incentive for this novel approach was his interest in sound generation in pipe organs. He found that these surfaces of discontinuity—vortex sheets—are highly unstable, this instability being the key element linking the continuous flow in the organ mouth to oscillating motion and sound. He showed as well how atmospheric convection cells at the planetary scale dissipate their energy in large vortices through the destabilization of sheared surfaces. In his pioneering article, Helmholtz states that “wherever an irregularity is formed on the surface of an otherwise stationary current, this must give rise to a progressive spiral unrolling of the corresponding part of the surface” but neither Helmholtz himself nor anyone to our knowledge ever published a description of this response to a localized perturbation. The goal of the present letter is to report this experiment and describe the self-similar growth we have observed.

The difficulty which Helmholtz encountered in quantifying mathematically the evolution of a localized perturbation opened the way for the successful approach which Kelvin made popular through his 1871 paper: small amplitude perturbations combined with sinusoidal initial conditions [2]. Indeed, the nonlinear/localized conception of Helmholtz is critically opposed to the linear/wavelike theory of Kelvin. The difference between these two approaches is illustrated in figure 1 where we see the response of a mixing layer to a localized initial perturbation (Helmholtz) and a wavelike initial perturbation (Kelvin).

For a detailed account of fluid mechanics in the times of

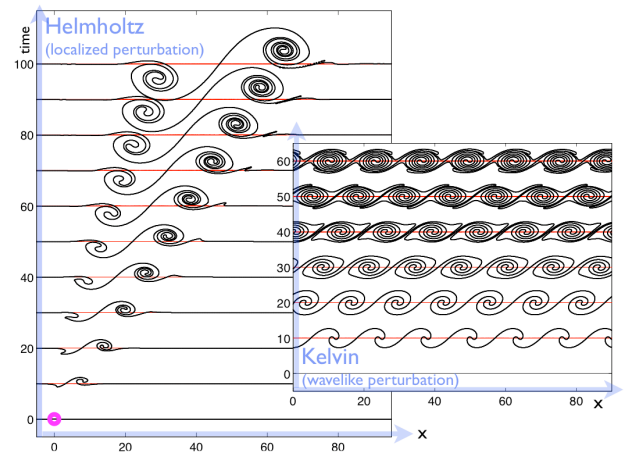


FIG. 1: Kelvin-Helmholtz instability excited by two types of initial perturbation, shown by the deformation of the interface. $We = 1000$, $Re = 100$. The two fluids have the same density ($r = 1$). For the wavelike initial condition, we observe the familiar roll-up of the interface in vortices whose size is fixed by the initially imposed wavelength. For the localized initial perturbation, we observe the creation of a system of two vortices growing in size without alteration in shape.

Helmholtz and Kelvin, see [3]. There has been a renewed interest for the mathematical analysis of vortex sheets, following the analysis by Moore [4] of the formation of a shape singularity in finite time. Also, for a review of singularities in fluid mechanics, see [5]. For a book on the dynamics of vorticity, see Saffman [6].

Our numerical experiment consists of a two-phase mixing layer with interface initially at height $y = 0$. The two fluids have the same viscosity ν , and density ρ_{gas} and $\rho_{liq} = 1$. The bottom fluid is at rest and the top fluid has free-stream velocity $U = 1$. Gravity is not included. Owing to viscosity, the shear profile varies continuously through the interface. We use an initial velocity profile in the form of an error function in the liquid and the gas,

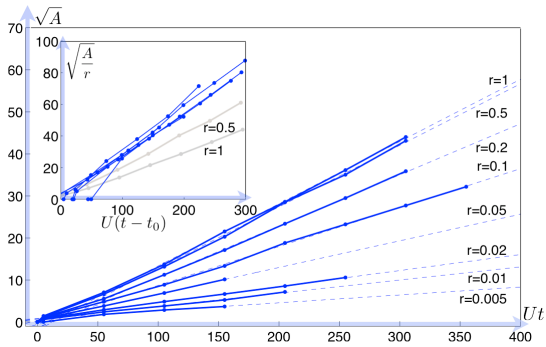


FIG. 2: Measured wave size $L = \sqrt{A}$ growing in time for several density ratios. We observe an algebraic growth of the wave. The speed of growth depends on the density ratio r : the lighter the gas, the slower the growth. As inset, we scale the growth with the law in square root of r according to the theoretical analysis $L \propto \sqrt{r}Ut$. The wave shapes for $r \neq 1$ are shown in figure 4.

with matching at the interface satisfying the stress continuity. The height of the mixing-layer is defined by the parameter $\delta = 1$ in both fluids. The Reynolds number for both fluids is $Re = U\delta/\nu = 100$, based on the mixing layer height and velocity difference. We will see that the density ratio $r = \rho_{gas}/\rho_{liq}$ will play a central role in the dynamics. The interface is characterized by its surface tension σ . The capillary resistance of the interface to aerodynamic deformation forces is quantified by the Weber number $We = \rho_{gas}U^2\delta/\sigma = 1000$.

We simulate the evolution of this system using the Navier–Stokes equations for a two-fluid system. The equations are discretized using a finite volume scheme, and the interface is traced in the framework of the volume of fluid method (VOF) [7]. The open source software *Gerris Flow Solver* is used which allows for octree adaptive grid refinement [8]. Results obtained with this code have been compared to stability theory for mixing layers in [9]. The refinement criterion is based on a combination of interface curvature and fluid vorticity with a smallest cell size of 0.0635. The numerical simulations are performed in a large domain (width 260, height 130) with periodic boundary conditions in the streamwise direction and symmetry boundary conditions at top and bottom. A perturbation is induced at initial time in the center of the domain, in the form of a localized upward force of extent $L_0 = 1$ and amplitude low enough such as to initiate the instability without creating a vertical jet.

A first quantitative description of the wave growth is given in figure 2. The size of the wave is measured from the simulation output as $L = \sqrt{A}$ with A the area of liquid which has crossed through the initial interface location $y = 0$. We observe an algebraic growth, whose slope decreases with the density ratio r .

Let us first ignore capillarity and viscosity. The evolving vorticity field for instance is parameterized as $\omega =$

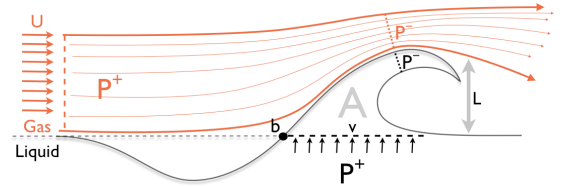


FIG. 3: Schematic representation of the wave as an obstacle to the gas stream. The acceleration of the gas stream above the wave induces a pressure drop. The pressure gradient $(P^+ - P^-)/L$ sucks liquid into the wave.

$\omega(x, y, t, U, \rho_{gas}, \rho_{liq}, \delta, L_0)$, function of the two spatial coordinates and time, as well as five parameters specifying the system and the initial excitation. There are three independent physical dimensions, ω can thus be written

$$\omega = \frac{U}{\delta} f\left(\frac{x}{Ut}, \frac{y}{Ut}, \frac{\rho_{gas}}{\rho_{liq}}, \underbrace{\frac{\delta}{Ut}}_{\rightarrow 0}, \underbrace{\frac{L_0}{Ut}}_{\rightarrow 0}\right)$$

where f is a dimensionless function. As the wave is growing, the inertial length Ut becomes arbitrarily larger than the initial mixing layer thickness $\delta/Ut \rightarrow 0$ which appears at the scale of the wave as a vorticity sheet. Similarly, the initial forcing appears as a Dirac; the vorticity thus becomes $(U/\delta)f(x/Ut, y/Ut, r, 0, 0)$ where time enters exclusively through the length scale: the wave is steady in the coordinates $x' = x/Ut, y' = y/Ut$; this is the self similar law. The density ratio r is the single remaining parameter.

We will see that the shape and phenomenology change very much with r . We can nevertheless attempt to derive a scaling for one particular wave property: its size L . For this we need to model the forces in balance. To this aim, an idealized wave anatomy is proposed in figure 3. In essence, the head of the wave is an obstacle to the gas stream, leading to an acceleration of the gas above. Thanks to self-similarity, the streamline pattern does not change in time, thus the speed above the wave remains proportional to U . We denote P^+ the ambient pressure, and P^- the low pressure above the wave. This low pressure is communicated to the liquid in the wave head as shown on the figure. The Bernoulli equation relating pressure and velocity in the gas yields $P^+ - P^- \propto \rho_{gas}U^2$ if we neglect the nonstationary terms. The same law applied inside the wave, gives $P^+ - P^- \propto \rho_{liq}v^2$, where v is the velocity at which the liquid feeds the wave. Since the pressure drop is the same in the liquid and the gas, we have $v \propto \sqrt{\rho_{gas}/\rho_{liq}}U$: the suction velocity v depends linearly on U and is impacted by the density ratio through a square root law. Note also that v is constant in time throughout the evolution of the wave, just like U .

We may now derive the evolution law for the wave size: the wave area A grows in time as liquid is sucked through

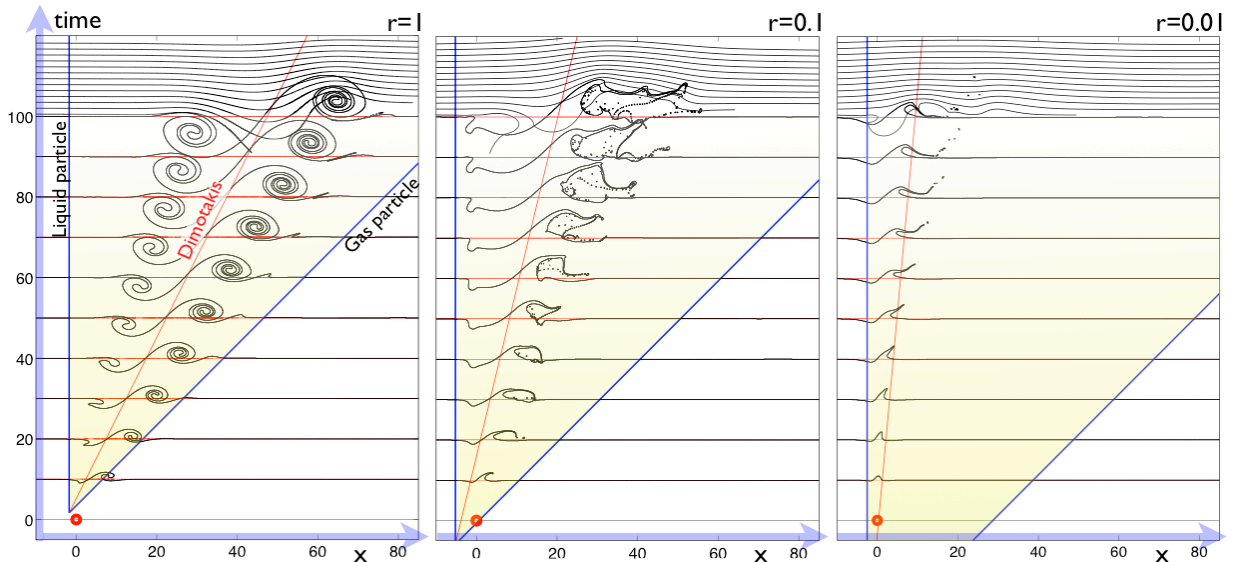


FIG. 4: Evolution of the wave represented as a spatiotemporal diagram for three representative density ratios. The characteristic cone delimited from the virtual origin by the liquid and gas speed is represented as a frame of reference. The speed of advancement of the wave is compared to the Dimotakis speed, characteristic of propagation in this two-phase system. The origin of the self-similar shape (x_0, t_0) is visualized as the tip of the characteristic cone. We observe that it differs from $(0, 0)$. This effect is due to the transient from the initial forcing.

its bottom of size L , thus $\partial_t A \propto Lv$. Also, $A \propto L^2$, and since v is a constant, we obtain a differential equation for the wave size $\partial_t L \propto v$, thus our final result

$$L \propto \sqrt{\frac{\rho_{gas}}{\rho_{liq}}} Ut.$$

This law is confronted against simulated data in the inset of figure 2 by drawing the measured \sqrt{A}/r as a function of Ut . We observe indeed collapse of the slopes for values of the density ratio up to 0.1. For two phases of similar densities ($r > 0.1$), our model anatomy is not representative: the wave tends to a symmetric shape with respect to $y = 0$ and cannot be reduced to an obstacle against the gas flow.

Based on dimensional analysis, we know that the wave cannot be self-similar if viscosity, capillarity or gravity is large compared to inertia, at least not self-similar in the way we describe in this paper. Capillarity imposes a minimum wave size: the wave cannot grow when it is so small that the fixed driving pressure drop $\rho_{gas}U^2$ is balanced by the capillary pressure jump σ/L across an interface with radius of curvature L . This lower bound is $L_{cap} \propto \sigma/\rho_{gas}U^2$. Viscosity will slow down the growth of small waves for which the driving is of the order of the Poiseuille pressure drop $\mu v/L$. Gravity on the other hand imposes a maximum size, that for which the hydrostatic pressure $\rho g L$ from foot to head equals the driving. This upper bound is $L_{grav} \propto rU^2/(1-r)g$. The self-similar wave solution is thus allowed as an intermediate asymptotics (see [10]) between the small capillary and viscous scales, and the large gravity scale. This intermediate range is made

comfortable for fixed fluid properties μ, σ, g by choosing an intense free-stream velocity. These results in terms of characteristic lengths can equivalently be expressed with the Reynolds, Weber and Froude numbers built on the wave size: the evolution of a wave of size L is self similar if $Re_L = \rho_{gas}UL/\mu > \sqrt{r}$, $We_L = \rho_{gas}U^2L/\sigma > 1$ and $Fr_L = U^2/gL < (1-r)/r$.

We now turn to the description of the wave shape as r varies. Being a self-similar shape, the wave has a virtual origin (x_0, t_0) . We measure t_0 by extrapolating back in time the algebraic law for its size. For the origin in space we need another robust characteristic of the wave: we chose the position of the point b at its back as shown on figure 3. The downstream location of this point is found to increase algebraically as the wave advances and grows; it can be extrapolated back in time to yield the location x_0 of the virtual origin. Figure 4 represents the evolution of the wave in time for three density ratios, in the form of spatiotemporal diagrams.

We now define the *characteristic cone*: it originates from the virtual origin and is delimited by two characteristic lines, the line of the fastest speed of the system—the speed of a gas particle—and the slowest speed in the system—that of a liquid particle. At equal density of liquid and gas ($r = 1$), the wave must be symmetric with respect to the point b as indeed observed. The wave is large and occupies most of the cone width. For smaller gas densities, the wave is asymmetric, with a shape resembling that of our model analysis. Its position remains close to the upstream limit of the cone: the wave grows slowly. Unlike gravity or capillary waves, this structure does not

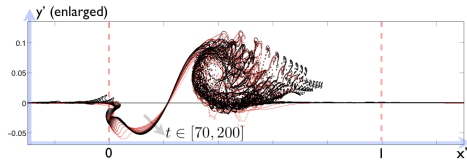


FIG. 5: Wave interface overlapped in time, recast in the self-similar reference frame (x', y') for density ratio $r = 0.1$. We can observe the self-similar shape of the wave, disturbed by instationarity at the wave tip and drop shedding. We see on figure 4 that the initial transient for $r = 0.1$ lasts until about $t = 70$.

propagate at its own phase speed, it merely grows, with its back pinned at the cone upstream edge. To provide a further velocity reference for the wave displacement, we have indicated the Dimotakis speed $V_D = U\sqrt{r}/(\sqrt{r} + 1)$ with a red line (see [11]).

The scaling law for the measured wave area is now verified. We must proceed to assess whether the complete shape grows homothetically. We make use once more of the virtual origin. The wave height and width are rescaled as $x' = (x - x_0)/U(t - t_0)$, $y' = y/U(t - t_0)$. The scaled wave interfaces are represented overlapped in time in figure 5 for $r = 0.1$.

The flow structure is represented in figure 4 by instantaneous streamlines at time $t = 100$. For $r = 1$ it consists in a pair of co-rotating vortices reminiscent of two consecutive vortices of the usual wavelike scenario, except that here the two vortices are not aligned horizontally (see figure 1 for a comparison). This configuration is reminiscent of the simultaneous roll-up of two semi-infinite vortex sheets into Kaden spirals (see [6]). When reducing the gas density—here for $r = 0.1$ —the upstream vortex no longer forms and is replaced with an elongated gas recirculation bubble. The downstream vortex also fails to roll gas and liquid together, but takes the form of a gas vortex sheltered from the main stream by the liquid body of the wave. The wave grows a tongue which undergoes flapping. Liquid drops are torn from the wave through this flapping motion, and sent partly off to the gas stream and partly into the vortex core. For still lower gas densities, $r = 0.01$, the wave grows much slower and is found pinned at the upstream limit of the characteristic cone. The tongue flaps and detaches from time to time; the liquid being now completely thrown out to the fast gas stream. We observe periodic detachment of the downstream vortex in a typical vortex shedding sequence. The streamline pattern of figure 4 shows two gas vortices: one is in the instance of leaving the shelter of the wave, and the second further downstream is the fruit of the previous shedding event.

This vortex shedding for low r is to our knowledge a new mechanism which the study of the self-similar wave allows to identify. Indeed, we understand now that the wave grows slowly for low r and that its back travels at

the speed of the liquid. There must thus be a qualitative transition when reducing r , toward a regime where the wave appears to the gas stream as a fixed obstacle, with the ensuing vortex shedding. The wave’s tongue is a fragile object, periodically teared into drops through the interaction of its own inertia and violent vortex departures. The ejection angle, drop size and frequency could be analyzed along the lines of this atomization scenario.

“Since a general solution must be judged impossible from wants of analysis, we must be content with the knowledge of some special cases, and that all the more, since the development of various cases seems to be the only way of bringing us at last to a more perfect knowledge.” (Euler in [13], cited from Craik [14]). The self-similar response of the Kelvin-Helmholtz instability to a localised perturbation may indeed be a special case in this spirit. The growth law in the square root of the density ratio $L \propto \sqrt{r}Ut$ was derived from an idealized wave anatomy. The quantitative success of this simple analysis tells that figure 3 depicts a realistic idealized configuration, ensuring that the underlying nonlinear mechanism for growth was indeed uncovered. We have described the intimate structure of the wave in figure 4, showing the mutations of the system of two vortices accompanying the liquid wave, and its impact on the dynamic behavior of the wave.

We are grateful to Marco Fontelos, Christophe Josserand and Sergio Chibbaro for comments on the manuscript.

* Electronic address: jerome.hoeffner@upmc.fr

- [1] H. Helmholtz, *Phil. Mag. series 4* **36**, 337 (1868).
- [2] W. Thomson, *Phil. Mag. series 4* **42**, 362 (1871).
- [3] O. Darrigol, *Worlds of flow* (Oxford university press, 2006).
- [4] D. W. Moore, *Proc. R. Soc. Lond. A.* **365**, 105 (1979).
- [5] J. Eggers and M. Fontelos, *Nonlinearity* **22** (2009).
- [6] P. G. Saffman, *Vortex dynamics* (Cambridge University Press, 1992).
- [7] G. Tryggvason, R. Scardovelli, and S. Zaleski, *Direct numerical simulations of gas-liquid multiphase flows* (Cambridge University Press, 2011).
- [8] S. Popinet, *J. Comp. Phys.* **228**, 5838 (2009).
- [9] D. Fuster, A. Bagné, T. Boeck, L. Le Moine, A. Leboissetier, S. Popinet, P. Ray, R. Scardovelli, and S. Zaleski, *Int. J. Multiphase Flow* **35**, 550 (2009).
- [10] G. I. Barenblatt, *Scaling* (Cambridge University Press, 2006).
- [11] P. E. Dimotakis, *AIAA J.* (1986).
- [12] H. A. Becker and T. A. Massaro, *J. Fluid Mech.* **31**, 435 (1968).
- [13] L. Euler, *Principes généraux du mouvement des fluides, Opera Omnia* (Clifford Truesdell(ed.), Lausanne, 1954), vol. 12 of *ser. 2*.
- [14] A. D. D. Craik, *Wave interactions and fluid flows* (Cambridge University Press, 1988).